Precision targeting tumor cells using cancer-specific InDel mutations with CRISPR-Cas9

Taejoon Kwon[a,b,1,2], Jae Sun Ra[a,1], Soyoung Lee[b,1], In-Joon Baek[a,c,1], Keon Woo Khim[d], Eun A Lee[a], Eun Kyung Song[d], Daniyar Otarbayev[a,b], Woojae Jung[a,d], Yong Hwan Park[a,3], Minwoo Wie[a,d], Juyoung Bae[b], Himchan Cheng[b], Jun Hong Park[a,4], Namwoo Kim[a,d], Yuri Seo[a,5], Seongmin Yun[b], Ha Eun Kim[d], Hyo Eun Moon[e], Sun Ha Paek[e], Tae Joo Park[a,d], Young Un Park[c], Hwanseok Rhee[c], Jang Hyun Choi[a,d], Seung Woo Cho[a,b,f,2], and Kyungjae Myung[a,b,2]

[a]Center for Genomic Integrity, Institute for Basic Science, Ulsan 44919, Republic of Korea; [b]Department of Biomedical Engineering, College of Information and Biotechnology, Ulsan National Institute of Science and Technology, Ulsan 44919, Republic of Korea; [c]Cascure Therapeutics, Ulsan 44919, Republic of Korea; [d]Department of Biological Sciences, College of Information and Biotechnology, Ulsan National Institute of Science and Technology, Ulsan 44919, Republic of Korea; [e]Department of Neurosurgery, Seoul National University Hospital, Seoul 03080, Republic of Korea; and [f]Korean Genomics Center, Ulsan National Institute of Science and Technology, Ulsan 44919, Republic of Korea

Edited by Philip Hieter, University of British Columbia, Vancouver, BC, Canada; received February 21, 2021; accepted January 21, 2022

An ideal cancer therapeutic strategy involves the selective killing of cancer cells without affecting the surrounding normal cells. However, researchers have failed to develop such methods for achieving selective cancer cell death because of shared features between cancerous and normal cells. In this study, we have developed a therapeutic strategy called the cancer-specific insertions–deletions (InDels) attacker (CINDELA) to selectively induce cancer cell death using the CRISPR-Cas system. CINDELA utilizes a previously unexplored idea of introducing CRISPR-mediated DNA double-strand breaks (DSBs) in a cancer-specific fashion to facilitate specific cell death. In particular, CINDELA targets multiple InDels with CRISPR-Cas9 to produce many DNA DSBs that result in cancer-specific cell death. As a proof of concept, we demonstrate here that CINDELA selectively kills human cancer cell lines, xenograft human tumors in mice, patient-derived glioblastoma, and lung patient-driven xenograft tumors without affecting healthy human cells or altering mouse growth.

CRISPR | insertion/deletion | cancer | double-strand breaks

Genomic instability is a hallmark of most cancers (1–3). The Pan-Cancer Analysis of Whole Genomes study of the International Cancer Genome Consortium and The Cancer Genome Atlas have identified the genomic instabilities most frequently found in tumors (4, 5). In addition to single-nucleotide mutations, most cancer cells contain somatic mutations, which are primarily small insertions and deletions (InDels) that do not exist in neighboring normal cells. Whole-exome sequencing of solid tumors revealed that ∼5% of the total somatic variation in cancer cells are InDels, thus suggesting that InDels can also be candidates for tumor-specific neoantigen immunotherapy (6). A more recent study that analyzed 2,658 whole-cancer genomes reported that most tumors had 100 to 1,000 InDels (5). Incorrect DNA repairs by nonhomologous end joining (NHEJ) or microhomology-mediated end joining (MMEJ) might be a major cause of InDel formation in proliferating tumors (7). Recently, other DNA repair pathways including transcription-coupled repair and mismatch repair pathways were also suggested, which have contributed to InDel formation in different cancer cells (8).

Conventional cancer therapies target uncontrolled cancer cell growth (9). Owing to the continuous DNA replication required for proliferation, DNA damaging agents that inhibit DNA replication have been used as part of many conventional cancer therapies, including radiation and chemotherapeutic regimens. However, these treatments also damage the DNA in neighboring healthy cells, which then causes undesirable side effects including cell death and mutations (10). Therefore, an ideal cancer therapy would only target features that are unique to cancer cells. Recently, selective cancer cell killing was reported in cells that were addicted to a mutation or a cancer-specific protein produced by chromosomal translocation. The mutation or translocation breakpoint junctions were targeted with CRISPR-Cas9 (11, 12). Although these novel approaches were used to achieve selective cancer cell death, they are not extensively applicable because it is difficult to identify critical mutations or fusion proteins produced by translocation in most cancer cells.

CRISPR-Cas9 is a bacterial native immune system that inhibits bacteriophage infection by inducing sequence-specific DNA double-strand breaks (DSBs) in the bacteriophage

Significance

The targeted killing of cancer cells without affecting surrounding normal cells is the most desirable approach for cancer therapy; however, it cannot be easily achieved, owing to the shared properties of normal and cancer cells. Using CRISPR-Cas9 targeting multiple cancer-specific mutations, we developed an innovative approach called cancer-specific insertions and deletions attacker that can induce targeted cancer cell death by simultaneous and multiple DNA double-strand breaks. As demonstrated in cell lines, cancer patient–driven cells and xenografts, the concept proposed in this study may become a potential approach for personalized cancer treatments.

Author contributions: T.K., J.H.C., S.W.C., and K.M. designed research; J.S.R., S.L., I.-J.B., K.W.K., E.A.L., E.K.S., D.O., W.J., Y.H.P., M.W., J.B., H.C., J.H.P., N.K., Y.S., S.Y., H.E.K., and Y.U.P. performed research; H.E.M., S.H.P., T.J.P., H.R., S.W.C., and K.M. contributed new reagents/analytic tools; T.K., J.S.R., S.L., I.-J.B., K.W.K., E.A.L., E.K.S., J.B., H.C., J.H.P., Y.U.P., H.R., J.H.C., S.W.C., and K.M. analyzed data; and T.K., S.W.C., and K.M. wrote the paper.

Competing interest statement: S.W.C., T.K., H.R., and K.M. are shareholders of CasCure Therapeutics, Inc.

This article is a PNAS Direct Submission.

[1]T.K., J.S.R., S.L., and I.-J.B. contributed equally to this work.

[2]To whom correspondence may be addressed. Email: tkwon@unist.ac.kr, swcho@unist.ac.kr, or kmyung@ibs.re.kr.

[3]Present address: School of Medicine, Ajou University, Suwon 16499, Republic of Korea.

[4]Present address: Herbal Medicine Resource Research Center, Korea Institute of Oriental Medicine, Naju 34054, Republic of Korea.

[5]Present address: Graduate School of Analytical Science and Technology, Chungnam National University, Daejeon 34134, Republic of Korea.

This article contains supporting information online at http://www.pnas.org/lookup/suppl/doi:10.1073/pnas.2103532119/-/DCSupplemental.

Published February 25, 2022.

genome (13). CRISPR RNA guides Cas9 endonuclease to specific DNA sequences in a bacteriophage to induce DNA DSBs. A DNA DSB is one of the most harmful types of DNA damage. A single unrepaired DSB can kill bacteria, and similar effects are predicted in other single-cell organisms including yeast (14–17). These drastic cell death effects in bacteria and yeast could be attributed to the preferential homologous recombination (HR) process to repair DNA DSBs. However, unlike bacteria and yeast, mammalian cells rely heavily on an alternative DSB repair pathway commonly referred to as NHEJ (18). NHEJ has two primary advantages for repairing sequence-specific DNA DSBs when compared with HR. First, NHEJ does not require a repair template. Thus, NHEJ can be used to repair DNA DSBs in all cell cycle phases. Secondly, owing to its mutagenic characteristics, NHEJ adds or removes nucleotides at the broken DNA site, thus destroying the enzymatic recognition sites used for sequence-specific DNA DSBs. Despite the improved repair pathway, mammalian cells still cannot tolerate high quantities of simultaneous DNA DSBs.

In this study, we developed a method called cancer-specific InDel attacker (CINDELA) that selectively kills cancer cells. CINDELA targets multiple InDel mutations produced during cancer development with CRISPR-Cas9 enzymes to only kill cancer cells. The CINDELA method was successfully applied to kill cancer cell lines, xenografted cancer cells in mice, patient-derived glioblastoma, and in a patient-driven xenograft (PDX) lung cancer model without affecting normal cells or mice.

Results

Induced Cancer Cell Death Based on Multiple Simultaneous DNA DSBs. We hypothesized that targeting InDels would produce high quantiles of cancer cell–specific DNA DSBs to kill cancer cells selectively (Fig. 1*A*). First, we tested whether enzymatically induced DSBs can be sufficient to kill proliferating cancer cells using ER-*Asi*SI U2OS cells. ER-*Asi*SI U2OS cells express the *Asi*SI restriction enzyme that translocates into the nucleus in the presence of tamoxifen (4OHT) (19) (Fig. 1*B*). The current version of the human genome (GRCh38) contains 1,225 *Asi*SI recognition sites. Given that only 10 to 20% of *Asi*SI recognition sites can be cut in vivo, owing to their epigenetic status of DNA methylation (20, 21), we predicted that ~100 to 200 DSBs can occur depending on the cell type. When *Asi*SI was translocated into the nucleus after 4OHT treatment, almost all the ER-*Asi*SI U2OS cells were dead compared with U2OS cells treated with 4OHT (Fig. 1*B*). The DNA DSB marker γ-H2AX and apoptosis were induced in ER-*AsisI* U2OS cells after 4OHT treatment (Fig. 1 *C* and *D*). These data demonstrated that large quantities of enzymatically produced DSBs can kill proliferating cancer cells.

To test whether DNA DSBs induced by CRISPR-Cas9 can also kill cancer cells, we selected well-known CRISPR-Cas9–targeting sequences that appear repeatedly that range from a single to 20,000 targets in the human genome (Dataset S1). We observed that human embryonic kidney cells (HEK293T) started to die when the number of synthetic guide RNA (sgRNA) targets increased to more than 10, which created 20 DSBs in the genomes of diploid cells (Fig. 2*A*). HEK293T cell death was further enhanced when the transfected plasmid expressed the sgRNA and targeted a higher number of genomic locations (Fig. 2*A*). We delivered the same, multiple-target sgRNA using a lentiviral delivery into other types of tumor cells: HCT-116, MDA-MB-231, and K562. When the cells were cultured in competitive conditions (22), we observed gradual increases in cell death when the sgRNA that targeted a higher number of genomic locations was expressed in all these cells (Fig. 2 *B* and *C*).

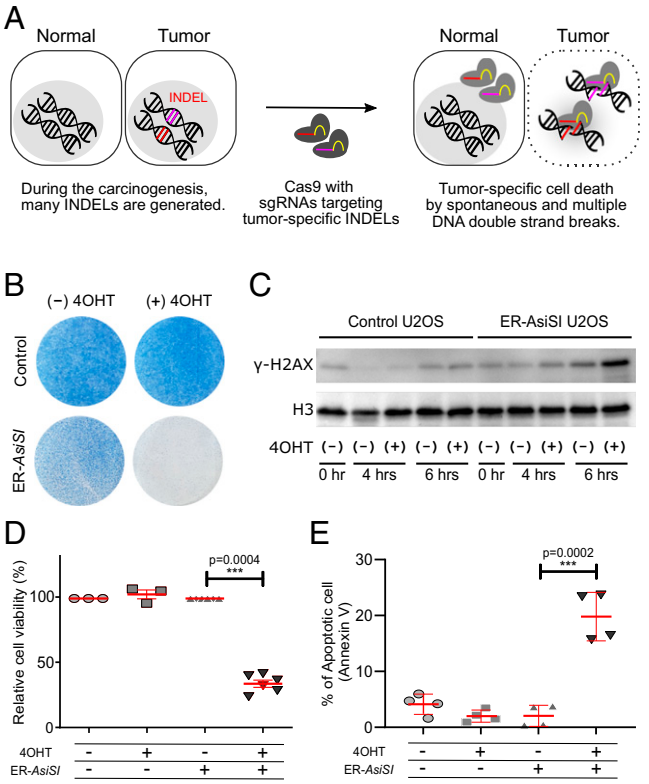

Fig. 1. CINDELA concept and cancer cell death induced by simultaneous multiple DSBs. (*A*) Schematic of the CINDELA approach. (*B*) Simultaneous, multiple DNA DSBs (generated with the restriction enzyme *Asi*SI) induced cell death in osteosarcoma cells (U2OS). (*C*) Time-dependent DSB occurrence caused by *Asi*SI localization confirmed by the signal of γ-H2AX. (*D*) The relative cell viability outcomes indicated that a significant number of cells died when *Asi*SI induced multiple DSBs. We quantified the cell viability and compared it with nontreated controls 6 d after the induction. *P* values were calculated using an unpaired Student's two-sided *t* test. (*E*) The proportion of apoptotic cells confirmed that multiple simultaneous DSBs induced active cell death. *P* values were calculated using an unpaired two-sided Student's *t* test.

To test whether DSBs at specific InDels produced by CRISPR-Cas9 can selectively kill cancer cells (CINDELA method), we determined whole-genome nucleotide sequences of U2OS and HCT-116 cells derived from osteosarcoma and colon cancer, respectively. For comparison, the whole genome of RPE1, a non-tumor cell line that originated from retinal pigment epithelium and immortalized by telomerase expression, was also sequenced. For the InDels identified in each cell line, we designed sgRNAs targeting cell line–specific InDels (see *Materials and Methods* and Datasets S2–S4 for details) and validated by in vitro cleavage (*SI Appendix*, Fig. S1). To investigate whether these sgRNAs can induce cell-specific DNA DSBs, we transfected 30 CRISPR-SpCas9 (*Streptococcus pyogenes* Cas9) ribonucleoprotein (RNP) complexes that targeted U2OS-specific InDels into U2OS cells. The death of U2OS cells with U2OS-specific, InDel-targeting CRISPR-RNP complexes began at 72 h post-transfection. No cell death was observed when HCT-116–specific, InDel-targeting CRISPR-RNP complexes were transfected into U2OS cells (Fig. 3*A*). Furthermore, dose-dependent cell death was observed when the number of guide RNAs (gRNAs) was reduced from 30 to 18, 12, or 6 for RNP delivery (*SI Appendix*, Fig. S2). We also delivered cancer cell–specific or multiple target sgRNAs in HCT-116 or U2OS cells using lentivirus. Unlike sgRNA targeting wherein either no-target or two-target loci were identified, sgRNA targeting affected 50 loci in the genome that killed both HCT-116

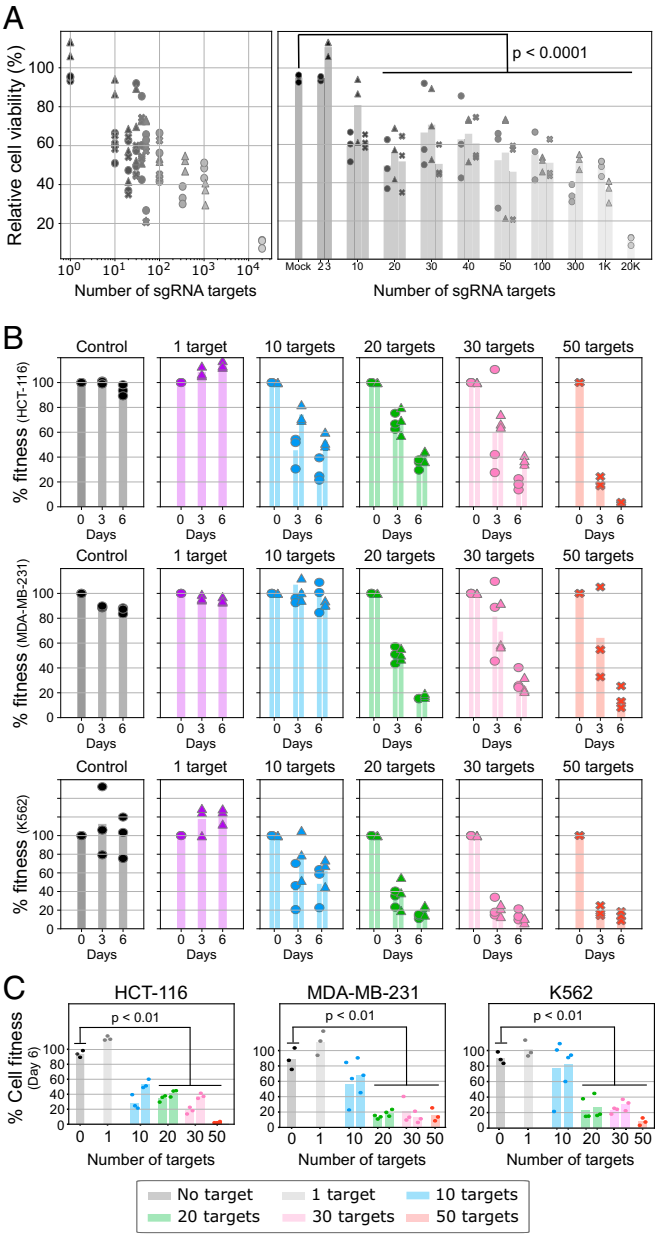

Fig. 2. Cancer cell death by simultaneous, multiple DSBs induced by CRISPR-Cas9 depends on the number of DSB targets. We designed CRISPR-Cas9 gRNAs that targeted multiple locations on the human reference genome (hg38), putatively producing from a single DSB target to 20,000 simultaneous DSB targets, and tested whether they can induce cell death depending on the number of induced DSBs. (*A*) The cell viability according to the number of DSB targets in HEK293T cells. Plasmids encoding multiple target gRNAs were transiently expressed in the HEK293T cells, and cell viability was measured by the CellTiter-Glo assay. It should be noted that different bars for a given number of sgRNA targets on *Right* (also presented on *Left*) represent distinctive gRNAs we designed with the same number of putative targets. (*B*) DSB-induced cell death in three different cell lines (HCT-116, MDA-MB-231, and K562). Lentivirus encoding the multiple target gRNA transduced each cell line stably expressing Cas9 protein. The cell fitness was measured based on the fraction of fluorescence protein encoded in lentivirus (see *Materials and Methods* for detailed procedure). (*C*) Statistical test (unpaired Student's *t* test) confirmed the significance of cell fitness loss when the cell has more than 20 simultaneous DSBs.

and U2OS cells (Fig. 3*B*). Similar to the actions of sgRNA with 50 targets, sgRNAs targeting of cell-specific InDels (23 InDels for HCT-116, 21 InDels for U2OS) killed these cells (Fig. 3*B*). An increase rate of cells with apoptotic signals and decreased cell viability were only observed in cells killed by CINDELA.

Because RNP complex delivery to the in vivo tumor environment is challenging, we also tested whether the CINDELA treatment can utilize the adeno-associated virus (AAV)-based *Staphylococcus aureus* Cas9 (SaCas9). For in vivo CINDELA testing, we produced AAVs that coexpressed both sgRNAs targeting cancer-specific InDels and SaCas9 (23). A total of 30 AAVs coexpressing different sgRNAs (UMIX30) and SaCas9 were transduced into U2OS cells (Fig. 3*C*). Selective U2OS cell death caused by AAVs targeted U2OS-specific InDels. Therefore, we conclude that similar to the transfection approach, AAV-transduced CINDELA also caused cell death (Fig. 3*C*).

CINDELA Treatments Selectively Kill Patient-Derived Primary Tumors. To prove that CINDELA treatment can be applied to actual tumor samples, we used the primary tumor cell line GBL-67 derived from a Korean glioblastoma patient. Based on whole-genome sequencing data, we designed 26 SaCas9 CINDELA gRNAs that targeted specific GBL-67 InDels. Because we did not have access to normal cells from the same individual, NSC-10 neural stem cells, which do not have the targeted InDels, were used as the control. AAVs expressing sgRNA and SaCas9 were generated and simultaneously transduced into primary glioblastoma GBL-67 and NSC-10 cells. We found that ∼50 cell-specific DSBs induced by CINDELA treatment were sufficient to enhance apoptosis and kill glioblastoma cells (Fig. 4*A*). In contrast, the NSC-10 cells did not exhibit any growth attenuation after the same transduction.

CINDELA Treatment Suppresses Xenograft Tumor Growth and PDX In Vivo. We subsequently tested whether CINDELA can inhibit in vivo tumor growth. We created a xenograft model with HCT-116 cells and injected lentivirus (2×10^7 viral particles/injection) with SpCas9 and sgRNA targeting multiple loci (MT2 for two loci, MT50 for 50 loci) or sgRNAs targeting HCT-116–specific 23 InDels (HMIX23) for 2 wk on a daily basis. As expected, lentiviral treatment of MT50 and HMIX23 significantly inhibited tumor growth compared with that of MT2 (Fig. 4*B*). When we treated higher titer lentivirus (2×10^8 viral particles/injection) expressing SpCas9 and MT50 sgRNA every 3 d for four times, the tumor sizes were not increased compared with the case in which the lentivirus was expressing SpCas9 and sgRNA with no predicted target locus (NT) (Fig. 4*C*). Mice did not show any prominent symptoms during lentiviral treatments, thus suggesting that lentiviral-delivered CINDELA did not affect normal mice tissues and cells.

U2OS cell xenografts were created in nonobese diabetic severe combined immunodeficient (NOD-SCID) mice and monitored until the tumor size reached ∼1 cm. Either AAVs expressing U2OS-specific CINDELA sgRNAs and SaCas9 or AAVs expressing only SaCas9 were then injected into the mice five times within a 3-d interval for 2 wk. As shown in Fig. 4*C*, we observed that tumor growth was selectively inhibited by the injection of the AAVs that expressed U2OS-specific CINDELA sgRNAs and SaCas9. The HA-tag of SaCas9 was detected in tumor sections from mice injected with a) SaCas9 only and b) with SaCas9 with sgRNAs (*SI Appendix*, Fig. S3*A*). Mice did not show any prominent symptoms during AAV treatment, which suggested that AAV-delivered CINDELA did not affect normal tissues and cells (*SI Appendix*, Fig. S3*B*). To check the specific cell death pathway induced by the CINDELA treatment, we harvested the remaining tumors and stained them for γ-H2AX or terminal deoxynucleotidyl transferase dUTP nick end labeling (TUNEL). As anticipated, CINDELA-targeted tumors led to a significant induction of γ-H2AX (Fig. 4*D*) and apoptotic cell death (*SI Appendix*, Fig. S3*C*) in addition to TUNEL signaling (Fig. 4*E*) when compared with control tumors.

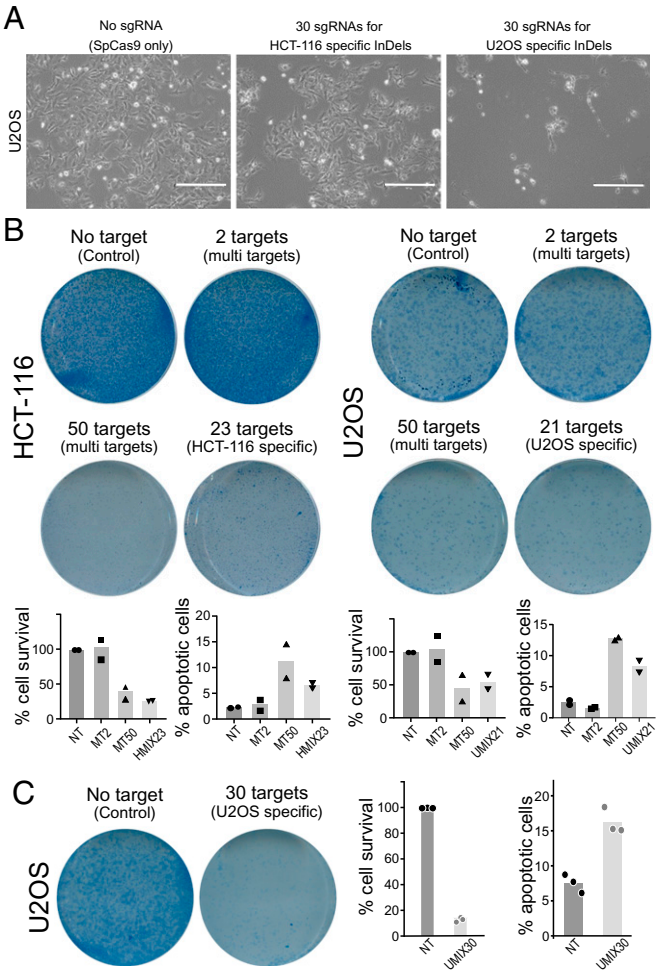

Fig. 3. CINDELA with CRISPR-Cas9. (*A*) CINDELA-induced cancer cell death introduced by the SpCas9 RNP complex with 30 gRNAs targeting U2OS-specific InDels. (Scale bar, 300 μm.) (*B*) CINDELA-induced cell death introduced by the lentivirus-delivered SpCas9. We tested by using multiple target gRNAs in conjunction with cell type–specific gRNAs (23 sgRNAs for HCT-116 and 21 sgRNAs for U2OS). The relative cell viability and the proportion of apoptotic cells confirmed the specific cell death by CINDELA both on multiple target gRNAs and cell type–specific InDel targeting gRNAs. (*C*) CINDELA-induced cell death introduced by the AAV-delivered SaCas9. When we pooled AAV with 30 different gRNAs targeting U2OS-specific InDels and SaCas9 and delivered it to U2OS cells. Compared with the control (with no gRNA), a significant number of cells died.

Lastly, we tested CINDELA's efficacy in PDXs, which are predictive preclinical models for cancer treatment (24). After sequencing tissue from an established lung cancer PDX, we identified ~30 CINDELA targets (29 gRNAs for SPX4-073 and 22 gRNAs for SPX4-318). Xenograft tumor size was monitored for 2 wk after the injection of AAVs (five times within a 3-d interval) that expressed SaCas9 with the targeted sgRNAs. PDX tumor growth was inhibited by the AAVs that expressed sgRNAs and SaCas9. In contrast, AAVs that only expressed SaCas9 did not inhibit tumor growth (Fig. 4*D* and *SI Appendix*, Fig. S4 *A* and *B*). In addition, the mice did not exhibit any significant symptoms during the AAV treatment (*SI Appendix*, Fig. S4*C*).

Discussion

Selective cancer cell killing is considered the best therapeutic strategy against cancer; however, the implementation has remained elusive. Inhibitors of DNA replication, DNA repair, and cell metabolism have been investigated as unique cancer cell targets (25). However, shared mechanisms between cancer and normal cells, including progenitor and stem cells, remain a considerable hurdle. In this study, we developed a method to induce targeted cancer cell death by utilizing CRISPR-Cas to introduce simultaneously multiple DNA DSBs. To overcome the risk of targeting the DSBs in normal cells, we focused on short InDels that CRISPR-Cas can distinctively recognize. In the future, an engineered CRISPR-Cas system with high fidelity (26, 27) can be used to achieve CINDELA targeting to single base-level changes with increased precision.

Cell death caused by multiple DSBs using CRISPR-Cas was previously reported as an unintended side effect of genome-wide CRISPR screens. Hart and colleagues reported that promiscuous gRNAs that targeted at least 20 genomic loci can introduce significant growth defects, similar to sgRNAs that targeted the essential genes (28). Similarly, genes with higher copy numbers exhibited strong lethal effects in the CRISPR screen, which can be considered as false positives (29, 30). In our experiments, CINDELA required ~10 to 30 sgRNAs to kill cancer cells, which is similar to previous reports. The requirement for such a high number of DSBs is primarily attributed to the highly effective NHEJ and potentially MMEJ DNA repairs in mammalian cells (31).

Cancer cells in tumors are heterogeneous, owing to the accumulation of mutations during their rapid proliferation. InDel mutations targeted by CINDELA can only affect a subset of the cancer cells in a tumor. Thus, the choice of the InDel mutations that need to be targeted is critical. Most abundant InDels, possibly generated at an early tumorigenesis stage, would likely be the most effective at irradicating the most abundant tumor population. Any cancer cells that survived through an initial CINDELA treatment can be retargeted by choosing additional InDel mutations in successive treatments.

Multiple sgRNA deliveries would be a critical part of the implementation of the CINDELA treatment. Although we could not directly measure the number of sgRNAs in each cell, a gradual increase in cell death with increased CINDELA sgRNAs was observed. In general, the cell death effect is directly attributed to increased DNA DSB events. However, different DNA repair capacities in different cancer cells can cause differential cell death effects. Acute cell death caused by the introduction of multiple DSBs follows an intact apoptotic cell death pathway in most cases. However, it is possible that several cancer cells, especially those carrying a p53 mutation, may require several days for cell death to occur, owing to the lack of proper apoptotic pathways. We speculate that multiple DNA DSBs may trigger a senescence type of cell death characterized by growth inhibition within these cancer cells. The detailed mechanisms of CINDELA-induced cell death should be investigated further.

Combinatorial treatment with other drugs, such as DNA DSB response inhibitors or other chemotherapeutic reagents, can be considered to enhance the efficiency of CINDELA methods. We tested the ATM inhibitor (KU60019) and cisplatin with CINDELA treatment and observed the synergistic improvement of specific cell death (*SI Appendix*, Fig. S5). Many inhibitors of NHEJ might also be beneficial to increase the DSB effect by CRISPR-Cas (32–34). PARP1 recognizes DNA DSBs in G1 cells to direct both NHEJ and strand-break repairs. PARP1 inhibitors are approved for clinical treatments of ovarian tumors. They undergo clinical trials for breast tumors that have lost the homologous recombination repair pathway (25). Thus, PARP1 inhibition might increase CINDELA's efficacy for cancer treatment.

In this study, we presented a therapeutic approach to selectively kill cancer cells with minimal side effects to healthy

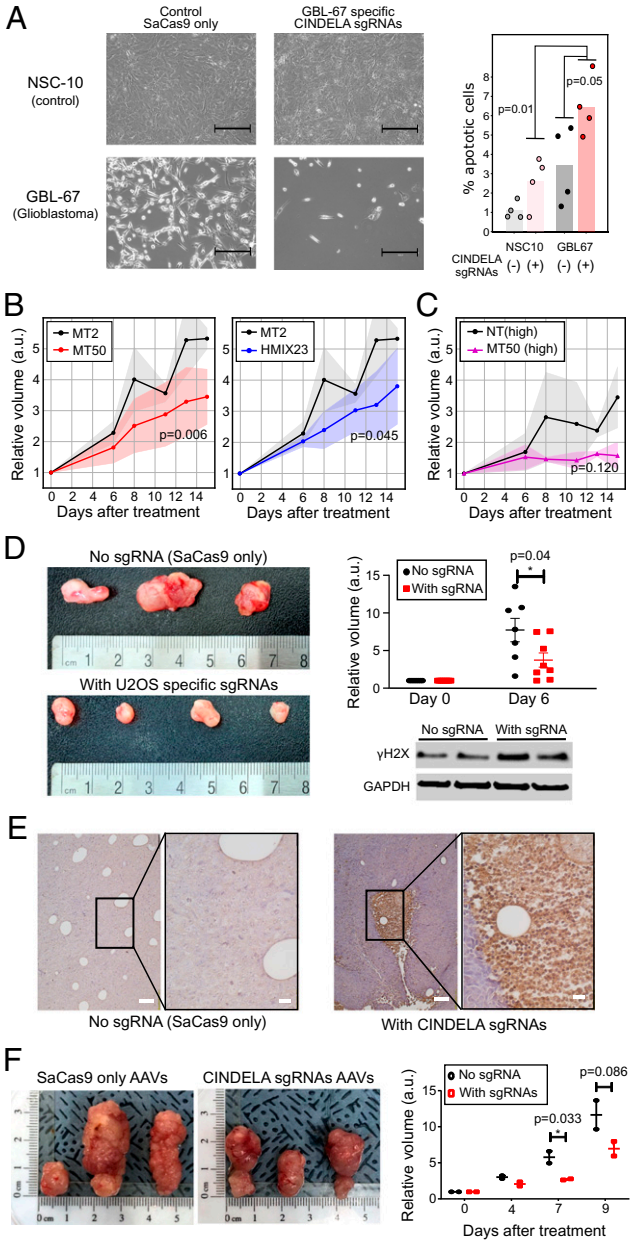

Fig. 4. In vivo CINDELA effects in a patient-derived cell line and a mouse xenograft model. (*A*) Primary tumor cells derived from a glioblastoma patient (GBL-67) were treated with 26 CINDELA sgRNAs and SaCas9 using AAV transduction. Compared with a neural stem cell line (NSC-10), the CINDELA treatment specifically killed GBL-67 cells. (Scale bar, 300 μm.) (*B*) We injected multiple target gRNAs (MT2 with two target loci, MT50 with 50 target loci) packaged with lentivirus (2×10^7 viral particles/injection) and observed a significant reduction of HCT116 xenograft. (*C*) High-titer lentivirus (2×10^8 viral particles/injection) with MT50 sgRNA enhanced tumor suppression. (*D*) Tumor growth was significantly delayed in tumors transduced with AAVs that expressed U2OS-specific CINDELA sgRNAs and SaCas9 compared with xenograft tumors that were transduced with AAVs expressing only SaCas9. Differences in relative tumor volume were analyzed using an unpaired two-sided Student's *t* test. (*E*) Increased apoptosis occurred in the xenograft tumor samples treated with CINDELA sgRNAs and SaCas9 compared with tumors treated only with SaCas9. The xenograft tissue was harvested 6 d after AAV injection, and cell death was measured with the TUNEL assay. (Scale bar, 100 μm [*Upper*], 20 μm [*Lower*].) (*F*) The lung cancer PDX model was treated with CINDELA sgRNAs and SaCas9. Remarkably, tumor growth was significantly delayed with CINDELA sgRNAs and SaCas9 treatment compared with the SaCas9 control (significance was tested with the use of a two-sided unpaired Student's *t* test).

cells using the CRISPR-Cas system. Most cancers have high mutational burdens. Therefore, our method is a practical cancer treatment that warrants consideration for future cancer therapy.

Materials and Methods

Cell Lines. We purchased the following cell lines from American Type Culture Collection (ATCC): HCT116 (CCL-247), U2OS (HTB-96), HEK293T (CRL-3216), and RPE1 (CRL-4000). Cells were cultured in Dulbecco's modified Eagle's medium (DMEM), which contained 10% fetal bovine serum (FBS) (General Electric ≥ Healthcare), 100 U/mL penicillin G (Life Technologies), and 100 μg/mL streptomycin (Life Technologies). The patient-driven glioblastoma cell line GBL-67 and neural stem cell NSC-10 were established and maintained (35) and used in this study following the approval of the Institutional Review Board (IRB) at the Seoul National University Hospital (IRB No. H-1904-117-1028). These cells were cultured in DMEM, which contained 20% FBS (GE Healthcare), 100 U/mL penicillin G (Life Technologies), and 100 μg/mL streptomycin (Life Technologies) in a 5% hypoxia chamber.

Cell Death Induced by Simultaneous Multiple DSBs Using *Asi*SI. U2OS cells with ER-*Asi*SI (19) were kindly provided as a gift by Tanya Paull (University of Texas at Austin, Austin, TX). ER-*Asi*SI U2OS cells were grown in DMEM, which contained 10% FBS (GE Healthcare). Subsequently, 1×10^5 cells were seeded into a 6-well plate, and 4-hydroxytamoxifen (4-OHT) (catalog [cat] no. H7904, Merck) was added to obtain a final treatment concentration of 300 nM. After 4 h of 4-OHT treatment, the media were refreshed, and the cells were incubated for 6 additional days. Cell survival was determined with either a colony-forming assay with methylene blue staining (cat no. M9140, Merck) or the CellTiter-Glo assay, performed according to the manufacturer's protocol (G9241, Promega).

Cell Death Caused by Simultaneous Multiple DSBs Using CRISPR. sgRNAs were designed to target multiple loci in the human genome with computational validation for their targets with the use of the Cas-OFFinder (36) against the human GRCh38 reference genome. Each sgRNA sequence was cloned into a sgRNA expression vector with a modified mouse U6 promoter from the pMJ179 plasmid (cat no. 85996, Addgene). A total of 1 d before transfection, 1.5×10^4 HEK293T cells were seeded in each well of a 96-well plate. Subsequently, 200 ng SpCas9 (cat no. 43945, Addgene) and sgRNA expression plasmids were transfected into the cells by using Lipofectamine 3000 (cat no. L3000015, Thermo Fisher Scientific). A total of 3 d post-transfection, cell viability was measured using the CellTiter-Glo Luminescent Cell Viability Assay (cat no. G7570; Promega) according to the manufacturer's instructions. Luminescence was measured using a microplate reader and Gen5 software (BioTek).

CINDELA gRNA Design. We performed whole-genome sequencing of cell lines and xenograft tissues using an Illumina NovaSeq 6000, which targeted 30× coverage with 150-base pair paired-end reads according to the manufacturer's instructions (Illumina). After trimming the adapter sequences with trimmomatic (version 0.39) (37), we mapped the reads against the human genome (GRCh38) with BMA-MEM (version 0.7.17-r1188) (38). The reads were mapped to the database with both human (GRCh38) and mouse (mm10) genomes. Filtered reads were then preferentially mapped to the human genome for further analysis with the xenograft samples. After removing the duplicated hits with Samtools (version 1.10) (39), we used Strelka2 (version 2.9.10) (40) with the default setting for calling germline variations. To design the sgRNAs for cancer cell line–specific InDels, we first filtered the InDels that had lengths equal to 3 to 8 bps and designed sgRNAs with those InDels for either SpCas9 or SaCas9. The heterogeneity, allele depth, and InDel availability in either the gnomAD database (version 2.1.1) (41) or other cancer cells we had previously tested were also considered when sgRNAs were prioritized. We checked the possibility of off targets using Exonerate (version 2.4.0) (42) with a two mismatch allowance, and all final candidate targets were visually inspected. All code used in this analysis is available on GitHub (https://github.com/taejoonlab/CINDELA-toolbox).

CINDELA Treatment with RNPs. We ordered the gRNAs that targeted cancer-specific InDels and the tracer RNAs (Integrated DNA Technologies). RNP complexes were formed by combining 20 μg equimolar mixture of tracer and gRNAs with 15 μg SpCas9 (43). We delivered RNPs with Lipofectamine CRISPRMAX Cas9 Transfection Reagent (cat no. CMAX00001, Thermo Fisher Scientific) according to the manufacturer's protocol.

CINDELA Treatment with Lentivirus. The lentiviral plasmid expressing CRISPR/SpCas9 under the EF1-α promoter (Addgene, no. 52962) was used to produce lentiviral production as described previously (22). Lentiviral particles were harvested on the third day after transfection into HEK293T cells and were

transduced to the K562, MDA-MB-231, or HCT-116 cell lines. For seven days, lentivirus-integrated cells were selected using blasticidin (concentration: 4 μg/mL) (Thermo Fisher Scientific, A1113903). After selection, clones were obtained by limiting dilution. High-titer lentiviral particles were purchased from the Vector Builder. The sgRNAs were cloned into modified murine U6 promoter-sgRNA-Puromycin-mCherry vector (modified from Addgene no. 46914), replacing the mCherry marker gene with BFP to monitor sgRNA expression. Lentiviruses with each sgRNA were produced and transduced to Cas9-expressing cell lines. In the cell fitness assay, puromycin selection (Thermo Fisher Scientific, A1113803) was performed to confirm sgRNA delivery (0.5 μg/mL for final concentration), and cells were then counted and mixed. The cell fitness was estimated by measuring the ratio of each fluorescence using flow cytometry cell sorting at days 0, 3, and 6 after the onset of the coculture.

CINDELA Treatment with AAV. The AAV plasmid expressing CRISPR/SaCas9 under the cytomegalovirus (CMV) promoter was purchased (Addgene, no. 61591). AAV virus particles were harvested on the third day after transfection into HEK293T cells and concentrated as described previously (44). The AAV serotype two was used for viral packaging, and 2.81×10^{10} viral particles were used to transduce target cells for CINDELA.

Xenograft and PDX Experiments. The nude or NOD-SCID mice were housed and maintained in standard conditions. All animal studies were performed with an approved protocol from the Institutional Animal Care and Use Committee (IACUC) of the Ulsan National Institute of Science and Technology (IACUC-19-05). Briefly, 6-wk-old mice were subcutaneously injected in one flank with 2×10^6 cancer cells. When the tumor size reached ~1 cm in length, the low-titer lentiviral particles were injected every day for 14 d. High-titer lentiviral or AAV particles were injected four times in 3-d intervals. A total of 2 wk after the primary injection, the tumors were harvested and analyzed. The TUNEL assay was performed using the Promega DeadEnd Colorimetric TUNEL System (cat no. G7360, Promega). PDX experiments were performed in DNA-link, Inc. (https://www.dnalink.com/) using previously described methods (45).

Cell Death Assay. The SaCas9 used in the AAV delivery was tagged with 3xHA and was detected with a monoclonal anti-HA antibody (cat no. H3663, Sigma-Aldrich). Cells with DNA damage were analyzed using an antiphospho-Histone H2A.X antibody that detected γ-H2AX (cat no. 05–636; Sigma-Aldrich). Apoptotic cell death was quantified using an Annexin V Alexa Fluor 488 conjugate (cat no. A13201; Thermo Fisher Scientific) and a BD FACSVerse instrument with the FlowJo software (version 10) according to the manufacturer's instructions.

Data Availability. The scripts used to analyze the InDels and design gRNAs are available at GitHub, https://github.com/taejoonlab/CINDELA-toolbox. Also, we deposited the InDels information at Dryad, https://doi.org/10.5061/dryad.9cnp5hqks. All other data are available in the main text or supplementary information.

ACKNOWLEDGMENTS. We thank members of the Center for Genomic Integrity, the Institute for Basic Science (IBS), and Dr. Jin-Soo Kim for helpful discussions and comments on the manuscript. We also thank Dr. Mooyoung Jung for his support of the project. This work is supported by IBS Grant IBS-R022-D1 (K.M., T.K., and S.W.C.), UNIST Research Fund (1.220023.01 to T.K. and 1.190041.01 to S.W.C.) and by a National Research Foundation of Korea Grant funded by the Korean Government Ministry of Science and ICT (Information & Communications Technology) (2020R1C1C1013242 to S.W.C.) and Ministry of Education (2018R1A6A1A03025810 to T.K.).

1. R. D. Kolodner, C. D. Putnam, K. Myung, Maintenance of genome stability in *Saccharomyces cerevisiae*. *Science* **297**, 552–557 (2002).
2. S. Negrini, V. G. Gorgoulis, T. D. Halazonetis, Genomic instability—An evolving hallmark of cancer. *Nat. Rev. Mol. Cell Biol.* **11**, 220–228 (2010).
3. D. Hanahan, R. A. Weinberg, Hallmarks of cancer: The next generation. *Cell* **144**, 646–674 (2011).
4. M. H. Bailey *et al.*; MC3 Working Group; Cancer Genome Atlas Research Network, Comprehensive characterization of cancer driver genes and mutations. *Cell* **173**, 371–385.e18 (2018).
5. ICGC/TCGA Pan-Cancer Analysis of Whole Genomes Consortium, Pan-cancer analysis of whole genomes. *Nature* **578**, 82–93 (2020).
6. S. Turajlic *et al.*, Insertion-and-deletion-derived tumour-specific neoantigens and the immunogenic phenotype: A pan-cancer analysis. *Lancet Oncol.* **18**, 1009–1021 (2017).
7. M. van Overbeek *et al.*, DNA repair profiling reveals nonrandom outcomes at Cas9-mediated breaks. *Mol. Cell* **63**, 633–646 (2016).
8. I. Georgakopoulos-Soares *et al.*, Transcription-coupled repair and mismatch repair contribute towards preserving genome integrity at mononucleotide repeat tracts. *Nat. Commun.* **11**, 1980 (2020).
9. V. T. DeVita Jr., E. Chu, A history of cancer chemotherapy. *Cancer Res.* **68**, 8643–8653 (2008).
10. S. M. Bentzen, Preventing or reducing late side effects of radiation therapy: Radiobiology meets molecular pathology. *Nat. Rev. Cancer* **6**, 702–713 (2006).
11. Z. H. Chen *et al.*, Targeting genomic rearrangements in tumor cells through Cas9-mediated insertion of a suicide gene. *Nat. Biotechnol.* **35**, 543–550 (2017).
12. T. Koo *et al.*, Selective disruption of an oncogenic mutant allele by CRISPR/Cas9 induces efficient tumor regression. *Nucleic Acids Res.* **45**, 7897–7908 (2017).
13. R. E. Haurwitz, M. Jinek, B. Wiedenheft, K. Zhou, J. A. Doudna, Sequence- and structure-specific RNA processing by a CRISPR endonuclease. *Science* **329**, 1355–1358 (2010).
14. S. E. Lee *et al.*, Saccharomyces Ku70, mre11/rad50 and RPA proteins regulate adaptation to G2/M arrest after DNA damage. *Cell* **94**, 399–409 (1998).
15. J. M. Pennington, S. M. Rosenberg, Spontaneous DNA breakage in single living Escherichia coli cells. *Nat. Genet.* **39**, 797–802 (2007).
16. D. Bikard, A. Hatoum-Aslan, D. Mucida, L. A. Marraffini, CRISPR interference can prevent natural transformation and virulence acquisition during in vivo bacterial infection. *Cell Host Microbe* **12**, 177–186 (2012).
17. L. Cui, D. Bikard, Consequences of Cas9 cleavage in the chromosome of *Escherichia coli*. *Nucleic Acids Res.* **44**, 4243–4251 (2016).
18. R. Scully, A. Panday, R. Elango, N. A. Willis, DNA double-strand break repair-pathway choice in somatic mammalian cells. *Nat. Rev. Mol. Cell Biol.* **20**, 698–714 (2019).
19. Y. Zhou, P. Caron, G. Legube, T. T. Paull, Quantitation of DNA double-strand break resection intermediates in human cells. *Nucleic Acids Res.* **42**, e19 (2014).
20. A. Canela *et al.*, DNA breaks and end resection measured genome-wide by end sequencing. *Mol. Cell* **63**, 898–911 (2016).
21. Y. Zhu *et al.*, qDSB-Seq is a general method for genome-wide quantification of DNA double-strand breaks using sequencing. *Nat. Commun.* **10**, 2313 (2019).
22. S. W. Cho *et al.*, Promoter of lncRNA gene PVT1 is a tumor-suppressor DNA boundary element. *Cell* **173**, 1398–1412.e22 (2018).
23. F. A. Ran *et al.*, In vivo genome editing using Staphylococcus aureus Cas9. *Nature* **520**, 186–191 (2015).
24. A. T. Byrne *et al.*, Interrogating open issues in cancer precision medicine with patient-derived xenografts. *Nat. Rev. Cancer* **17**, 254–268 (2017).
25. M. J. O'Connor, Targeting the DNA damage response in cancer. *Mol. Cell* **60**, 547–560 (2015).
26. B. P. Kleinstiver *et al.*, High-fidelity CRISPR-Cas9 nucleases with no detectable genome-wide off-target effects. *Nature* **529**, 490–495 (2016).
27. C. A. Vakulskas *et al.*, A high-fidelity Cas9 mutant delivered as a ribonucleoprotein complex enables efficient gene editing in human hematopoietic stem and progenitor cells. *Nat. Med.* **24**, 1216–1224 (2018).
28. T. Hart *et al.*, High-resolution CRISPR screens reveal fitness genes and genotype-specific cancer liabilities. *Cell* **163**, 1515–1526 (2015).
29. A. J. Aguirre *et al.*, Genomic copy number dictates a gene-independent cell response to CRISPR/Cas9 targeting. *Cancer Discov.* **6**, 914–929 (2016).
30. R. M. Meyers *et al.*, Computational correction of copy number effect improves specificity of CRISPR-Cas9 essentiality screens in cancer cells. *Nat. Genet.* **49**, 1779–1784 (2017).
31. Z. Mao, M. Bozzella, A. Seluanov, V. Gorbunova, Comparison of nonhomologous end joining and homologous recombination in human cells. *DNA Repair (Amst.)* **7**, 1765–1771 (2008).
32. M. D. Canny *et al.*, Inhibition of 53BP1 favors homology-dependent DNA repair and increases CRISPR-Cas9 genome-editing efficiency. *Nat. Biotechnol.* **36**, 95–102 (2018).
33. R. Jayavaradhan *et al.*, CRISPR-Cas9 fusion to dominant-negative 53BP1 enhances HDR and inhibits NHEJ specifically at Cas9 target sites. *Nat. Commun.* **10**, 2866 (2019).
34. T. Maruyama *et al.*, Increasing the efficiency of precise genome editing with CRISPR-Cas9 by inhibition of nonhomologous end joining. *Nat. Biotechnol.* **33**, 538–542 (2015).
35. J. E. Han *et al.*, Inhibition of HIF1alpha and PDK induces cell death of glioblastoma multiforme. *Exp. Neurobiol.* **26**, 295–306 (2017).
36. S. Bae, J. Park, J. S. Kim, Cas-OFFinder: A fast and versatile algorithm that searches for potential off-target sites of Cas9 RNA-guided endonucleases. *Bioinformatics* **30**, 1473–1475 (2014).
37. A. M. Bolger, M. Lohse, B. Usadel, Trimmomatic: A flexible trimmer for Illumina sequence data. *Bioinformatics* **30**, 2114–2120 (2014).
38. H. Li, Aligning sequence reads, clone sequences and assembly contigs with BWA_-MEM. arXiv [Preprint] (2013). arXiv:1303.3997 (Accessed 16 December 2021).
39. H. Li *et al.*; 1000 Genome Project Data Processing Subgroup, The sequence alignment/Map format and SAMtools. *Bioinformatics* **25**, 2078–2079 (2009).
40. S. Kim *et al.*, Strelka2: Fast and accurate calling of germline and somatic variants. *Nat. Methods* **15**, 591–594 (2018).
41. K. J. Karczewski *et al.*; Genome Aggregation Database Consortium, The mutational constraint spectrum quantified from variation in 141,456 humans. *Nature* **581**, 434–443 (2020).
42. G. S. C. Slater, E. Birney, Automated generation of heuristics for biological sequence comparison. *BMC Bioinformatics* **6**, 31 (2005).
43. S. Kim, D. Kim, S. W. Cho, J. Kim, J. S. Kim, Highly efficient RNA-guided genome editing in human cells via delivery of purified Cas9 ribonucleoproteins. *Genome Res.* **24**, 1012–1019 (2014).
44. Addgene, AAV production in HEK293T cells. https://www.addgene.org/protocols/aav-production-hek293-cells/. (Accessed 30 October 2019).
45. H. Y. Jung *et al.*, PDX models of human lung squamous cell carcinoma: Consideration of factors in preclinical and co-clinical applications. *J. Transl. Med.* **18**, 307 (2020).